CERTIFICATION BY SIMULATION OF AN EVTOL: CREDIBILITY ANALYSIS OF SIMULATION MODEL USING UNCERTAINTY QUANTIFICATION

Lorenzo Favaro
Politecnico di Milano
Milan, Italy

Agata Rylko
Politecnico di Milano
Milan, Italy

Giuseppe Quaranta
Politecnico di Milano
Milan, Italy

ABSTRACT

A methodology to assess the credibility of flight simulation models for certification by simulation is developed. Aim of the research is to determine if the model, despite its uncertainties, can reliably predict handling quality compliance for specific flight tasks. Applied to a lift+cruise VTOL model performing a deceleration-to-hover manoeuvre, this is achieved by quantifying the impact of input parameter uncertainties on predicted handling qualities and evaluating the envelope of the resulting uncertain aircraft transfer functions – scaled by a confidence ratio – against maximum unnoticeable added dynamics boundaries. While longitudinal dynamics largely remained within MUAD limits, indicating model's credibility for those aspects, vertical axis dynamics coupled with longitudinal inputs in some uncertain configurations exceeded these limits, correlating with observed flight test variability. This work ultimately presents a structured approach to model uncertainty quantification for HQ certification by simulation, bridging the gap between model input uncertainty and prediction confidence, and supporting safer VTOL development.

NOTATION

*

Symbols

A Rotor disk area, m^2

C_j Aerodynamic coefficients, -

C_{j_p}, C_{j_q} Derivatives due to roll/pitch rate, -

$C_{j\alpha}$ Derivatives due to angle of attack, -

C_{j_0} Zero attitude aerodynamic coefficients, -

C_T Thrust coefficient, -

D VTOL-enclosing diameter, m; Total drag force, N

h Altitude, m

H_{add} Added dynamics transfer function

I_x, I_y, I_z Moments of inertia, kg·m^2

I_{xy}, I_{xz}, I_{yz} Products of inertia, kg·m^2

K_T Dimensional thrust coefficient, kg·m

L Total lift force, N

M Margin, -; Mass, kg

M_l, M_m Rolling/pitching moment, N·m

p Roll rate, deg/s

q Pitch rate, deg/s

R Rotor radius, m

S_i First-order sensitivity index, -

S_{T_i} Total effect sensitivity index, -

T Rotor thrust, N

T_u Velocity scaling factor (LUT thrust-speed dependence), -

u_j Uncertainty due to j-source errors

U Total uncertainty

V Variance

V_{lon} Longitudinal velocity input, m/s

V_{wind} Wind speed, m/s

V_Z Vertical velocity, m/s

X_Z Vertical displacement, m

α Angle of attack, deg

ζ Damping, -

ζ_p, ζ_z Pole/zero damping, -

η Normalized coordinate along the PC1-direction, -

θ Pitch angle, deg

μ^* Modified mean of the Elementary Effects

ρ Air density, kg/m^3

σ Standard deviation of the Elementary Effects

τ_d Rotors' delay, s

τ_p Phase delay, s

ϕ Roll angle, deg

ψ Yaw angle, deg

ψ_{wind} Wind direction, deg

Ω Rotor angular speed, rad/s

ω_{BW} Bandwidth frequency, rad/s

ω_{dp} Dipole frequency, rad/s

ω_{n} Natural frequency, rad/s

ω_{180} Crossover frequency, rad/s

add Added

inp Input

lon Longitudinal

min Minimum

num Numerical

pk Peak

r Referent

*

Acronyms

ACAH Attitude Command/Attitude Hold

ACR Applicable Certification Rule

AD Atmospheric Disturbances

aHQs Assigned Handling Qualities

CbS Certification by Simulation

CHR Cooper-Harper Rating

CR Confidence Ratio

CS Certification Specification

DOE Design of Experiments

EASA European Union Aviation Safety Agency

EE Elementary Effects

eTF Envelope of Uncertain Transfer Functions

eVTOL Electric Vertical Take-Off and Landing

FCs Failure Conditions

FCS Flight Control System

FFT Fast Fourier Transform

FS Flight Simulator

FSM Flight Simulation Model

FTM Flight Test Manoeuvre

HQs Handling Qualities

HQR Handling Quality Rating

LHS Latin Hypercube Sampling

LUT Look-up Table

MC Monte Carlo

MHQRM Modified Handling Qualities Rating Method

MOAT Morris One-at-a-Time

MoC Means of Compliance

MUAD Maximum Unnoticeable Added Dynamics

MTE Mission Task Element

NFE Normal Flight Envelope

PCA Principal Component Analysis

PC1 First Principal Component

pHQs Predicted Handling Qualities

PIO Pilot-Induced Oscillation

QoI Quantity of Interest

qLPV Quasi-Linear Parameter Varying

SA Sensitivity Analysis

TF Transfer Function

TPR Transient Peak Ratio

UA Uncertainty Analysis

UAM Urban Air Mobility

UQ Uncertainty Quantification

VBD Variance-Based Decomposition

VTOL Vertical Take-Off and Landing

INTRODUCTION

Integrating vertical take-off and landing (VTOL) vehicles into urban airspace comes with enormous challenges from a design and technological standpoint and considering the necessary certification efforts. Demonstrating compliance with the flight-related airworthiness rules set by aviation authorities is indeed one of the most critical phases of the vehicle development process, even more so in the context of Urban Air Mobility (UAM): the evidence collection and compliance demonstration processes, which is primarily based on flight testing activities, is highly complex, time-demanding and require a lot of effort to minimise safety risks while keeping the representativeness of the flight test. Therefore, appropriate means of compliance (MoC) and guidelines for the certification of this class of vehicles are still under development. In this regard, in the publication of the MoC for the SC-VTOL Standard, the European Union Aviation Safety Agency (EASA) in MOC VTOL.2500(b) states that flight simulators ”may also support some certification tests” (Ref. 1), explicitly allowing the possibility of exploiting simulators as an alternative to flight tests under specific conditions and when appropriate measures are taken.

VTOL Handling Quality Regulatory Framework

The certification of aircraft configurations, which differ from conventional rotorcraft or fixed-wing aircraft, requires special care. The EASA decided to tackle the unique characteristics of these aircraft that have distributed lift/thrust units through the definition of a complete set of dedicated technical specifications in the form of a special condition for VTOL-capable aircraft, which culminated in the publication by the EASA of Special Condition for Small-Category VTOL Aircraft (SC VTOL) (Ref. 2). The topic of VTOL HQ certification takes on particular importance because adequate HQs lead to a limited pilot workload and sufficient spare capacities that provide full situational awareness and so a higher level of safety. To this aim, three specific rules of the SC-VTOL deal directly with HQs: VTOL.2135 Controllability, VTOL.2140 Control Forces, and VTOL.2145 Flying Qualities.

To show compliance with these rules, EASA proposed as a MoC the Modified Handling Qualities Rating Method (MHQRM) (Ref. 1) where the applicant must demonstrate reaching a minimum acceptable HQ rating for each flight phase and condition that has a probability of being encountered greater than 10^{-9}. The suggestion is to use the well-established Cooper-Harper Handling Qualities Rating (CHR) Scale (Ref. 3), but applicants may choose other scales. The probability of a flight condition is defined by a combination of individual probabilities associated with

- the **Flight Envelope** (Normal, Operational, Limit) the VTOL operates in;
- possible aircraft **Failure Conditions** (Nominal up to Major, Hazardous);
- the level of **Atmospheric Disturbances** acting on the vehicle, from total absence of AD up to those exciting structural limits (Light, Moderate, Severe).

EUROCAE ED-295 (Ref. 4) provides some guidance on how to collect the evidence required by the MHQRM. Inspired by the concept of Mission Task Element (MTE) of (Ref. 5), ED-295 developed a set of guidelines specifically tailored for VTOLs in the form of Flight Test Manoeuvres (FTM) to be performed with the pilot-in-the-loop. For each FTM the document proposes a set of limits, in terms of desired or adequate performance, that are quantitative measures, specifically tailored to the FTM under study, and aimed at identifying performance deficiencies. Furthermore, a subjective CHR must be provided by properly trained test pilots; it is therefore a pilot-assigned evaluation, similarly to (Ref. 5), where it is defined as Assigned HQs. The performance parameters serve to validate the pilot ranking, as they should correspond to the CHR assigned by the pilot.

Certification by Simulation Approach

With the term Certification by Simulation (CbS), we refer to all cases where flight simulation can be used to support, augment or replace flight testing in the demonstration of certification compliance ”without sacrificing the level of safety” (Ref. 6). This approach has been systematised for the certification of rotorcraft under EASA CS-27 and CS-29, as described in (Ref. 6). The process presented in (Ref. 6) is a structured, requirement-based methodology that begins with the definition of the Applicable Certification Rule (ACR) and progresses through the simulation-related phases necessary to develop a complete simulation ecosystem. This ecosystem includes the Flight Simulation Model (FSM), the Flight Simulator (FS), and the flight test activities designed to collect validation data for both the FSM and the FS. In the development of FSMs it is crucial to validate the models by evaluating the error in comparison with tests showing that they have a sufficient level of fidelity that translates into an error that is below a certain set of tolerances agreed with the certification authority. However, for certification activities, this is typically not enough, because the models can be used in conditions that cannot be compared with equivalent tests, so it is also necessary to provide evidence of the credibility of the models. The concept of credibility of the predictions made by simulations is somewhat elusive, but it expresses the level of confidence that the users of the FSM have in the fact that the results obtained with the FSM reflect the behaviour of the real aircraft. In (Ref. 6) the credibility is managed by the definition of a *confidence ratio* CR that is the ratio between the value of the distance between the performance obtained by the FSM and the performance limit allowed for the certification, called the margin M, and the uncertainty U in the prediction of that performance:

$$CR = \frac{M}{U} \tag{1}$$

where the uncertainty U collects the experimental uncertainty, the uncertainty of input data and parameters of the model, and the numerical uncertainty associated with the method used to solve the mathematical models.

Basically, the users accept that the higher the risk of using the model for certification, defined through the combination of the influence level and the predictability level (see (Ref. 6) for more details), the higher the confidence ratio CR must be (in any case greater than 1). In this way, asking for a margin $M = CR \cdot U$ to be significantly higher than the uncertainty, it is possible to ensure that the predictions have a higher degree of credibility.

The concept of a confidence ratio allows us to keep the credibility of models at the required level; however, it applies only to situations where there is a quantified requirement. In case of ACRs that rely on subjective pilot evaluations based on discrete – and often nonlinear (Ref. 12) – rating scales, such as the CHR, other criteria must be defined to assess credibility. Since this is exactly the case of HQs certification for VTOLs, this paper will try to extend the concept of CR proposed in (Ref. 6) to this case, exploiting the concept of MUAD Maximum Unnoticeable Added Dynamics to assess if the modification of the aircraft's dynamics due to uncertainties can or cannot be perceived by a pilot.

Proposed Approach for Credibility Assessment of a FSM

The first step of a credibility assessment is always composed of the validation and fidelity assessment of the FSM. In principle, since the ACRs in this case require performing a pilot-assigned evaluation, i.e., assigned HQ tests, it is the fidelity of these evaluations that should be the objective of the fidelity assessment and uncertainty quantification. However, we must acknowledge that any quantity measured during these tests will be affected not only by the FSM but also by the Flight Simulator characteristics and by the test pilot characteristics. As such, it will not represent a measure pertaining solely to the FSM quality. A different approach could be defined by making use of the concept of predicted HQs (pHQs) - obtained through an open-loop flight test and therefore related to the intrinsic flying qualities of the aircraft defined in (Ref. 5). They are chosen as a way to anticipate how an aircraft will behave in terms of HQs and in (Ref. 5) used as support for aircraft design, as it is possible to show that helicopters that have certain pHQs are expected to reach a certain level of Handling Quality Rating (HQR) in the aHQ tests. Similar behaviour may be expected for VTOLs. Consequently, an FSM of a VTOL can be considered a faithful (i.e., credible) reproduction of the real aircraft if it demonstrates pHQs that are sufficiently close to those measured during flight tests. At the same time, it is possible to assess the level of uncertainty of the FSM by looking at the uncertainty that results in the pHQs.

However, once the uncertainty on the pHQs of the FSM is quantified, it is necessary to understand how it translates into an uncertainty for the aHQs and how the confidence ratio could be taken into account. The paper will show that the impact of the uncertainty on the pHQs can be used to identify the configurations that will mostly affect the HQR that is obtained performing the MTE with the modified FSM. Additionally, to exploit the idea of confidence ratio, the process we suggest here is as follows:

- Select among the uncertain configurations those that lead to the worst pHQs.
- Compute the Transfer Functions (TFs) for these worst configurations and compare them with the nominal TFs obtained with the reference model.
- Define new TFs that are the nominal TFs plus the difference between the worst-case TFs and the nominal ones, multiplied by the confidence ratio (CR).

If the difference between the nominal TFs and the worst-case TFs multiplied by the CR stays within the range of mismatches that proved unnoticeable to pilots, defined as MUAD (Maximum Unnoticeable Added Dynamics) in (Ref. 13), it is possible to assume that the results obtained by using the nominal FSM must lead to assigned HQ ratings that have a sufficient degree of credibility. If this is not the case, i.e., the worst-case TFs are beyond the MUAD limits, the model developer has two options.

- Improve the models to reduce the uncertainty and/or reduce the uncertainty in the flight test measures.
- Perform several flight simulator test campaigns using nominal and worst-case models to quantify the impact of uncertainties on the rating for the aHQ.

Of these two options, the former should be the preferred option whenever possible. The latter, in fact, may require a large number of simulated flight tests. To verify whether this approach is feasible, we will start in this work by investigating the relationship that exists between the uncertain models that present the worst pHQs and the corresponding assessment of the aHQs. To avoid blurring the evaluation with subjective pilot evaluations, it has been decided to apply the approach to a drone model in which pilots are replaced by a virtual system that controls the aircraft. So, no flight simulator tests are presented here.

The paper is organised as follows: after defining the manoeuvre to be performed and describing the aircraft model, the uncertainty quantification analysis is presented to identify the relationship between the uncertainty of the input data and the resulting pHQs. Then, a first set of assigned HQ tests is presented, considering both the reference model and several modified models selected to represent the worst configurations, followed by an analysis of how the transfer functions of the worst cases compare with the MUAD boundaries. Finally, conclusions are drawn.

Applicable Certification Requirement

Given the width of the class of VTOLs currently under development, the Performance Standards and the intended manoeuvre should be consistent with the aircraft's specific features. To tailor the prescribed requirements to the specific vehicle, ED-295 (Ref. 4) conceives its performance standards in a parametric manner, through a scaling technique which defines the expected performance and precision to perform the task based on the eVTOL size. The scaling process is formulated using the *D-value*, which "*represents the diameter of the smallest circle enclosing the VTOL aircraft projection on a horizontal plane [...]*" a quantity defined in the SC-VTOL (Ref. 2); in this work, given the size of the VTOL (see Table 2), a value of 3 m has been selected to scale the test course task and requirements.

For this exercise, it has been decided to focus on a symmetric manoeuvre performed at low speed, so the chosen FTM is the *Deceleration to Hover*, a manoeuvre representative of the final approach to landing that a VTOL is typically expected to perform and during which good HQ should be considered essential for a safe flight. Figure 1 shows the test course setup.

According to ED-295 (Ref. 4), deviations of up to 10 ft ($\approx$ 3 m) are allowed to meet desired performance, which appears too loose in this case, considering the small size of the eVTOL. Given that this is the only requirement not affected by the scaling procedure, the altitude limits are here revised, reducing the threshold to 3 ft ($\approx$ 1 m) for desired and 6 ft ($\approx$ 2 m) for adequate performance. To evaluate the success of the FTM and the level of performance standards achieved, the requirements in Table 1 hold.

Table 1. Deceleration to Hover FTM Performance Criteria (Ref. 4).

Description	Desired	Adequate
Maintain lateral track within $\pm X$ meters from ground reference line	$\pm 0.3D$	$\pm 0.6D$
Maintain the heading within $\pm X$ degrees	± 10 deg	± 15 deg
Maintain radar altitude within $\pm X$ feet	3 ft	6 ft
The aircraft must be brought to a controlled hover within X meters of the intended endpoint. Overshoots are not permitted	$0.6D$	$0.6D$

VTOL AIRCRAFT DESCRIPTION

The aircraft under analysis is a small-scale unmanned eVTOL, designed, manufactured, and tested in flight by the Aerospace Systems and Control Laboratory (ASCL) of the Department of Aerospace Science and Technology at the Politecnico di Milano (DAER) (Refs. 15–17) (depicted in Figure 2). Featuring a lift + cruise configuration, it has two distinct sets of rigid propellers for thrust generation: eight fixed-pitch, variable-RPM three-bladed propellers are responsible for controlling the vehicle in helicopter mode, during take-off and landing and low-speed manoeuvres (using differential thrust), while a couple of two-bladed propellers produce forward thrust in aeroplane mode. The baseline structure is of a fixed-wing UAV, which features a small-sized fuselage and two rectangular wings with zero built-in twist. The EASA developed SC-VTOL for passenger transport with a maximum take-off mass of 3175 kg (Ref. 2) (up to nine passengers). However, in the context of this research, it has been decided to perform the certification exercise on a laboratory small-scale prototype to allow for a direct comparison with data from experimental tests. The main geometry and performance characteristics are detailed in Table 2.

The FSM is built on a Simulink-based platform using a component-based quasi-linear parameter-varying (qLPV) modelling approach, covering the full VTOL flight envelope. It includes a flight dynamics block simulating 6-DOF rigid-body motion with aerodynamic, propulsive, and gravitational effects, and a control unit structured in four cascaded loops. Aerodynamic forces are computed from numerical data via interpolated coefficients; stall and propeller–airframe interactions are not modelled. Propulsion is modelled using wind tunnel-based look-up tables, excluding motor dynamics. The control system uses PID and proportional controllers, with different modes to simulate pilot assistance. For certification, the VTOL operates in position mode, enabling control over ground speed, vertical velocity, and yaw via prescribed inputs.

Table 2. eVTOL main specifications.

Parameter	Value	Unit
Cruise speed	15	m/s
Stall speed	11	m/s
Maximum speed	22	m/s
Max gross weight	7	kg
Wing and fuselage span	3.12	m
Wing chord	0.25	m
Wing incidence	4.5	deg
Horizontal stabiliser span	0.721	m
Horizontal stabiliser chord	0.13	m
Horizontal stabiliser arm	1.08	m
Vertical propeller diameter	0.178	m
Vertical propeller chord at 80% radius	0.0124	m

UNCERTAINTY ANALYSIS FRAMEWORK

As described in (Ref. 6), validation and verification activities during FM development should eliminate or reduce all known error sources to acceptable levels, that is, below the sufficiency threshold established in agreement with the certification authority. What remains will be by its nature not known and can be quantified in terms of uncertainty. This uncertainty, in turn, will provide a tool to assess the credibility of the model also in the conditions where it is necessary to use the FSM to perform a prediction because no flight data are available to perform a validation. The total uncertainty, used in the CR expression Equation (1), is considered the combination of three sources (see (Ref. 6)):

- Uncertainty due to numerical errors u_{num};
- Uncertainty due to experimental errors (present only in the validation cases where the model is compared with experiments) u_{r};
- Uncertainty due to input errors u_{inp}, (i.e. to an erroneous knowledge of the parameters used as input for the FSM).

In the case analysed in this work, numerical models should be considered verified up to a level where the numerical error has been brought to values at least an order of magnitude smaller than the other sources of error. At the same time, we will

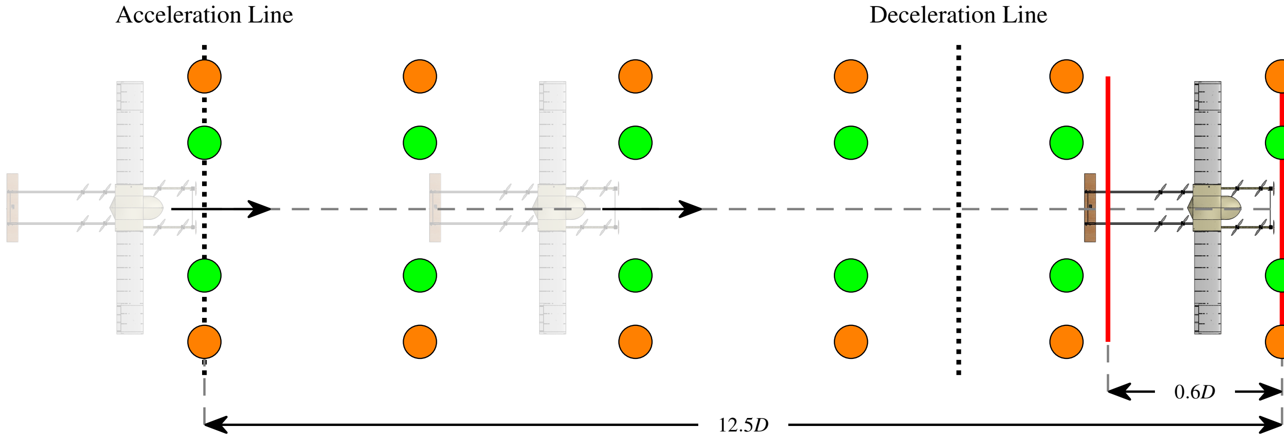

Figure 1. Deceleration to Hover Test Course, adapted from (Ref. 4).

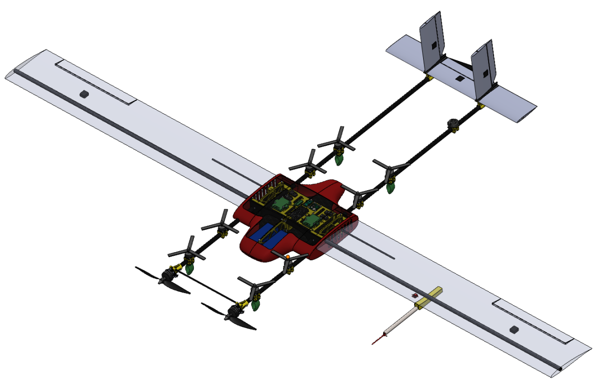

Figure 2. eVTOL CAD model overview.

not investigate the experimental error since we do not have experimental data to compare with, but we will concentrate on the assessment of the input errors, presenting the hypothesis that this part is the determining component of the total error. At this stage, we will present the hypothesis that all the uncertainties associated with input parameters are epistemic and not aleatoric. Most of them are the result of a lack of knowledge, due also to limited chances to have accurate experimental methodologies to measure them, more than a true, intimate aleatoric nature, which may be presented but often to a lower extent. Additionally, even for the cases where the aleatoric nature may appear as the best description, we often lack experimental measures capable of capturing the appropriate probabilistic characteristic for such parameters. In contrast, the usage of epistemic uncertainties requires only the definition of ranges of uncertainties that can be assessed in many cases using engineering judgement.

So, the uncertainty analysis presented here starts from the definition of epistemic uncertainty ranges for the most relevant parameters of the FM model and continues with the usage of efficient methodologies that may lead to quantifying the impact of these combined uncertainties on a set of well-chosen predicted handling qualities that are considered indicative of the performance that may be expected from the eVTOL drone in performing the deceleration-to-hover assigned handling quality test described in the previous section.

FSM–Dakota Coupling for Uncertainty Analysis

To achieve the HQ certification goal, the work aims at characterising the role and the implications of uncertainty on VTOL flight dynamics model. In this scenario, a statistical simulation tool was needed to wrap the existing FSM and to perform a series of Design of Experiments (DOE) analyses. The DOE aims to rank the uncertain input factors and quantify to what extent each of them affects the output quantities of interest (QoIs).

Due to its flexibility and ease of use, Dakota — a state-of-the-art software for uncertainty quantification, model calibration, and optimisation — was the natural choice, offering a wide range of variance-based and sensitivity analysis methods for DOE, along with meta-modelling capabilities for building surrogate models (Ref. 20). The latter is especially well-suited for integration into the eVTOL virtual simulation environment, especially for complex, time-demanding iterative analyses.

In principle, any analysis to propagate the uncertainty in the input parameters through the model to its output can be performed using Monte Carlo (MC) analysis (Ref. 21). However, when the number of parameters is large, the well-known "curse of dimensionality" may easily lead to intractable problems. Sensitivity analysis (SA), especially if performed with approximate models that use limited resources, may be used as a tool to determine which of the input factors can be fixed anywhere in the range of variation without significantly affecting the output and which are instead primarily influential (Ref. 22). Furthermore, in cases where all input parameters are defined in terms of intervals given their epistemic nature, a global SA may be all that is needed to perform a UQ analysis since it provides the range of variability of the output (Ref. 6). Several SA techniques are available in the literature (Ref. 23). Since each method shows advantages and drawbacks, a hybrid, comprehensive UQ framework is proposed and tested here (Ref. 24).

Morris One-at-a-Time Method

The first technique employed is the Morris one-at-a-time (MOAT) method (Ref. 25), which allows us to discern whether an input factor has a negligible, linear and additive, or nonlinear interaction effect on the model output. This approach evaluates the influence of each parameter, which can take only a discrete set of values called levels, by varying them individually along predefined trajectories: a trajectory consists of $k+1$ points, where k represents the number of model inputs. At each step along a trajectory, only one input variable is modified relative to the previous step, following a "one-at-a-time" variation approach. This process enables the computation of elementary effects (EEs) as the ratio of the incremental change in the output caused by the modified input. The EE values are then averaged, yielding to two key sensitivity indices: the modified mean μ^* and the standard deviation σ of the EE distribution. A high μ^* indicates that a factor has a strong overall impact on output, while a high σ indicates the presence of either nonlinear effects in the response or significant interactions with other factors. For additional details on the meaning of μ^* and σ, the reader should refer to (Ref. 22).

Variance-Based Decomposition

The MOAT method is conceptually simple and convenient to use when the number of factors is large and the computational time to elaborate the output is significant. However, it is used primarily for preliminary SA and does not explicitly isolate potential interaction effects among the FSM inputs arising from nonlinearities. A more quantitative evaluation is provided by Variance-based Decomposition (VBD) methods, which, as described in (Ref. 22), enable ranking inputs "according to the amount of output variance that is removed when we learn the true value of a given input factor." To achieve this, it is crucial to distinguish between first-order and total-effect contributions. The first-order index serves as a measure of the importance of an individual factor and, in a purely additive model, represents the exact proportion of the total variance attributed to that factor. This is quantitatively expressed through Sobol's main-effect index S_i. However, if the total variance V of the output Y cannot be fully explained by the sum of the first-order effects alone, interactions between input variables must be considered, as follows

$$V(Y) = \sum_i V_i + \sum_i \sum_{j>1} V_{ij} + \ldots + V_{12\ldots k} \qquad (2)$$

where $V(Y)$ is the total output unconditional variance. For the factor X_i, the Sobol index $S_i = \frac{V_i}{V(Y)}$. Computing high-order interaction terms $V_{12\ldots k}$ is often impractical for SA purposes. The computation of the total effect index S_{T_i} - which aggregates both the first-order effect of a factor and all its interactive contributions - represents a valid alternative

$$S_{\mathrm{T}_i} = S_i + \sum_{j \neq i} S_{ij} + \sum_{j \neq i} \sum_{l \neq i} S_{ijl} + \cdots \qquad (3)$$

The total effect index accounts for the total contribution to the output variation due to factor i, including the first-order effect and all higher-order effects due to interactions. This metric is widely recognised in the literature as a standard SA index and has shown a strong correlation with the MOAT method's μ^*, making it a useful basis for comparative analysis between methods. For a detailed discussion about VBD, the reader is again referred to (Ref. 22).

Proposed Multimodal Approach

To reduce the number of FSM executions, the problem is first tackled qualitatively, performing a preliminary analysis using the MOAT method, which gives a first characterisation of the most influential parameters. Then, a VBD quantitative analysis follows; however, performing a full VBD directly on the FSM would require an excessively high number of MC simulations. Hence, a surrogate model is developed for each pHQ QoI, generating an input-output dataset through Latin Hypercube Sampling (LHS) and constructing a meta-model that emulates the full behaviour of the FSM through Kriging Interpolation. By leveraging a limited set of simulations, Kriging exploits spatial correlations between sampled points to predict the value of the response function at unsampled locations. This results in an efficient computational emulator that can replace the original FSM, ultimately enabling the VBD and the computation of Sobol' indices. Figure 3 presents an overview of the methodology adopted. Information about Dakota's implementation of the methods can be found in (Ref. 26).

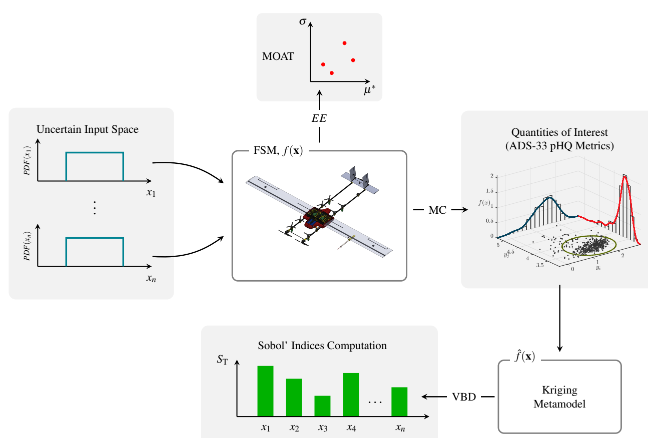

Figure 3. Uncertainty analysis workflow.

LOW-SPEED PREDICTED HQS: UNCERTAINTY ANALYSIS RESULTS

The analysis begins with the SA and UQ phases, hereafter jointly referred to as uncertainty analysis (UA), to investigate the relationship between the uncertainty of the FSM input data and the output u_{inp} identified through selected pHQ quantities of interest. This analysis is structured over two levels:

- By means of a preliminary SA, the key parameters in driving pHQ output uncertainty are identified, providing an insight into the model's dependence upon input parameters, including possible nonlinear/interaction effects arising throughout the simulations;
- Relying on UQ techniques, the effect of input space uncertainties on the selected pHQs is assessed and the related output uncertainty is quantified.

Focusing on the deceleration-to-hover FTM, four QoIs are identified in (Ref. 5) (this document is often colloquially identified as "ADS-33", making reference to the original design standard from which it originates (Ref. 27)). pHQs are selected as the corresponding fidelity metrics to characterise the longitudinal dynamics behaviour of the VTOL:

1. Roll-due-to-pitch coupling for aggressive agility (Section 3.3.9.2 of (Ref. 5));
2. Moderate amplitude pitch attitude changes (Section 3.3.3 of (Ref. 5));
3. Short-term response to pitch control inputs (Section 3.3.2.1 of (Ref. 5));
4. Mid-term response to pitch control inputs (Section 3.3.2.3 of (Ref. 5)).

In the following section, the main results of the UA are presented, highlighting the challenges encountered and the solutions proposed.

FSM Input Uncertainty Definition

The first step in the UA process is the characterisation of the uncertainties related to model input parameters. Table 3 summarises the main FSM factors to which an uncertainty range has been assigned, chosen to ensure sufficient coverage of the different building blocks within the FSM — following its component-based nature — from design parameters to aerodynamic characteristics.

Starting from roll-due-to-pitch coupling UA, no assumption on the possible decoupling between the longitudinal and lateral dynamics was made, hence generating $n = 22$ input factors comprehensive of VTOL's mass and inertia parameters (namely M, pitch inertia moment I_y and cross-inertia moment I_{xy}), aerodynamic coefficients and stability derivatives related to the longitudinal dynamics and vertical rotors' characteristics, including thrust coefficient K_T - defined as $K_T = C_T \rho A R^2 = T/\Omega^2$ based on (Refs. 14, 15) - rotors' thrust dependence on the longitudinal speed T_u (modelled as a gain on the airspeed information fed by the FSM sensor unit to the thrust-related LUT, to not influence thrust dependence on throttle command) and a time-delay on rotors' response to controller inputs. Since preliminary coupling analysis showed that there were no significant off-axis effects, the inter-axis factors (I_{xy}, the rolling moment terms $C_{M_{l_i}}$ and the roll rate terms C_{j_p}) were discarded in the subsequent analyses, reducing the uncertain input space to $n = 14$ dimensions.

Table 3. Uncertain Input Factors for UA Pitch Test.

Factor	Value	Range	Unit
M	7	± 0.5	kg
I_y	0.7237	$\pm 10\%$	kg·m^2
K_T	$6.96 \cdot 10^{-8}$	$\pm 15\%$	kg·m
T_u	1	$\pm 5\%$	-
τ_d	0	$+0.03$	s
C_{L_0}	0.7745	$\pm 20\%$	-
C_{D_0}	0.0183	$\pm 20\%$	-
$C_{M_{m0}}$	-0.0240	$\pm 20\%$	-
C_{L_α}	5.1270	$\pm 20\%$	-
C_{D_α}	0.2558	$\pm 20\%$	-
$C_{M_{m\alpha}}$	-0.5402	$\pm 20\%$	-
C_{L_q}	7.6136	$\pm 20\%$	-
C_{D_q}	0.7179	$\pm 20\%$	-
$C_{M_{mq}}$	-16.169	$\pm 20\%$	-

Uncertain ranges for each class of factors are assigned following a separate reasoning, given their intrinsic differences: aerodynamic and stability terms are derived from their nominal values, with a 20% increase/decrease applied. Similarly, I_y, K_T and T_u are defined in percentage terms, limiting their range of variability to avoid divergent simulations; rotors' delay τ_d follows the same logic. The mass range varies in both directions by 0.5 kg.

Moderate-Amplitude Pitch Attitude Changes

The first pHQ studies the attitude quickness, that aims "to characterise the helicopter's ability to achieve rapid, precise attitude changes when performing sharp, moderate amplitude manoeuvres" (Ref. 28). Given the dynamics and control architecture of the VTOL under study, a new interpretation of the requirement was necessary for two main reasons. The first concerns the input specification: ADS-33 suggests applying a step in the longitudinal cyclic for attitude command/attitude hold (ACAH) response types, or a pulse for rate response types (Ref. 29). In this case, since a positive control input ΔV_{lon} causes a pitch-down movement and the vehicle returns to its previous trim state after command release (similar to an ACAH-flown helicopter), a step input was deemed as the most suitable for the test. The second challenge involves defining the output metrics: ADS-33 requires the attitude change "to be made as rapidly as possible from one steady attitude to another" (Ref. 5), extracting two key quantities from the response, which are the ratio of the peak angular rate to the peak attitude change $q_{\text{pk}}/\Delta\theta_{\min}$ and the minimum attitude excursion before settling at the new trim state $\Delta\theta_{\min}$. However, due to the small pitch angles at which the VTOL flies, after the step input and its corresponding $\Delta\theta_{\text{pk}}$, the vehicle reaches a new trim without any undershoot, making $\Delta\theta_{\text{min}}$ difficult to identify clearly. In this study, by examining the recorded q time history, $\Delta\theta_{\text{min}}$ is then taken as the angle reached when the angular rate approaches the second stationary point after injection of the input, as shown in Figure 4.

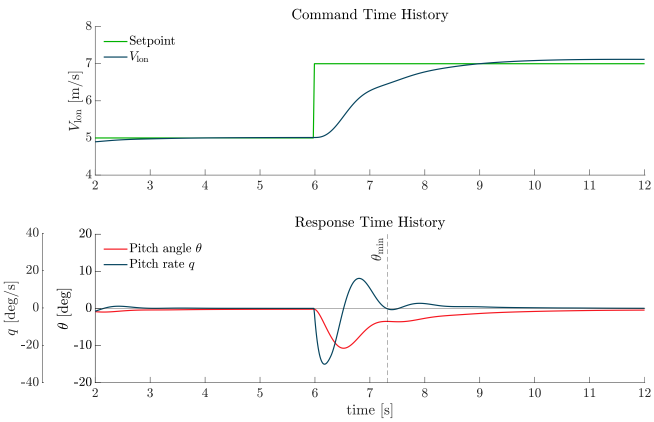

Figure 4. Attitude quickness test manoeuvre.

Focusing on MOAT results, Figures 5 and 6 display the modified mean μ^* against the standard deviation σ of the computed EEs as in (Ref. 30). The parameters located in the lower right-hand area behave mostly monotonically/linearly and appear to be highly significant in driving the model's behaviour, but without significant interactions with the other uncertain variables. On the other hand, those placed in the upper left-hand region show a high nonlinear/interactional effect. To compare factors and assess their relative importance, the criterion based on μ^* is selected; alternatively, the Euclidean distance from the origin in the $\mu^* - \sigma$ plane could be used (Ref. 23). Figure 5 shows $\Delta\theta_{\text{min}}$ MOAT results: almost all factors behave monotonically, with few or no nonlinearities/interactions. Moreover, a large number of them seem to affect the output measure, from mass to aerodynamic parameters. Indeed, aerodynamics plays a primary role. All lift-related coefficients are present, with a predominance of C_{L_0} and C_{L_α}. Pitching-moment stability derivatives appear too, together with drag-related ones; among the others, I_y and K_T prevail.

For the quickness metrics (Figure 6), the distinction between parameters becomes clearer: the eVTOL is mainly guided by mass and rotor-related factors, with response delay τ_d assuming a bigger role; as for aerodynamics, only C_{L_0} and C_{L_α} are visible (the other terms are relegated to low-order impacts).

In Figure 7, main and total effect indices for both pHQ metrics are shown (the threshold of 10^{-2} is indicated in the figure to easily discriminate the relevant factors), yielding good agreement with the MOAT results: both methods identify M, I_y, K_T and aerodynamic terms, also confirming the importance of C_{L_0}, C_{L_α} and $C_{M_{mq}}$.

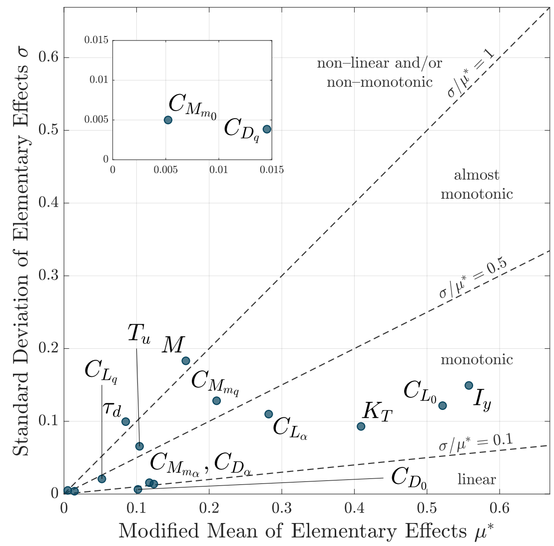

Figure 5. MOAT $\Delta\theta_{\text{min}}$.

Figure 8 shows the results of the MC analysis in the attitude quickness requirement plane. Most of the variability is located close to the high part of the y-axis, in the 2.5-3.5 1/s range. Due to the small dimensions of the aircraft, the results significantly exceed the HQ Level 1 limits prescribed by ADS33 for classical helicopters. This was expected and should not be considered indicative of the expected good HQs of the drone here under analysis, because the pHQ limits provided by (Ref. 5) must be considered as design indications only for the specific vehicle for which they have been drawn, which are manned helicopters.

Mid-Term Response to Pitch Control Inputs

The requirement of Section 3.3.2.3 in (Ref. 5) assesses the dynamic stability of the vehicle by looking at the eigenvalues - derived from the q-response to a ΔV_{lon} pulse input - in the complex plane. Figure 9 shows typical time histories. As per (Ref. 5), "the portion of the time history used to calculate the damping ratio should occur after the input is completed, and thus the initial oscillation caused by the pulse is disregarded. Additionally, since the damping ratio must be measured from the free response, concerns arose regarding the onboard attitude and rate controllers quickly restoring the trim state. To minimise their influence, the damping ratio ζ was evaluated using the Transient Peak Ratio (TPR) method (Ref. 5), considering only the first peak and first valley. The second positive peak was used to compute the characteristic period and the natural frequency ω_{n}.

Two main trends emerge from ζ results in Figure 10. Firstly, aerodynamics plays a greater role than in the quickness case, since C_{L_0} and $C_{M_{mq}}$ rank among the factors with the highest μ^*. Secondly, a high σ stems from M and τ_d, suggesting possible nonlinearities or interactive effects between variables.

Regarding the natural frequency ω_{n}, the MOAT method identifies three groups in the $\mu^* - \sigma$ plane: the first dominated

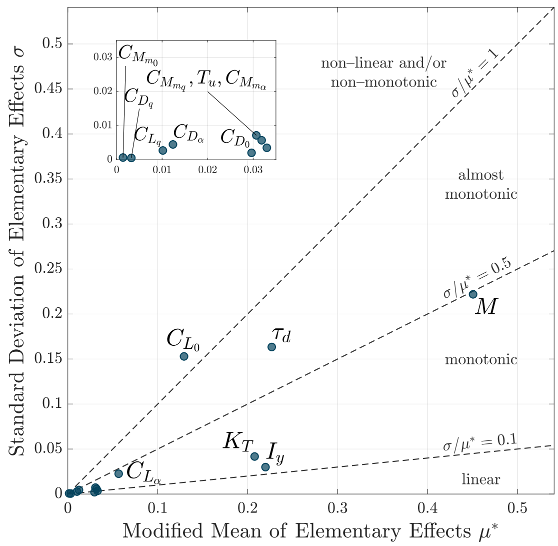

Figure 6. MOAT $q_{\text{pk}}/\Delta\theta_{\text{min}}$.

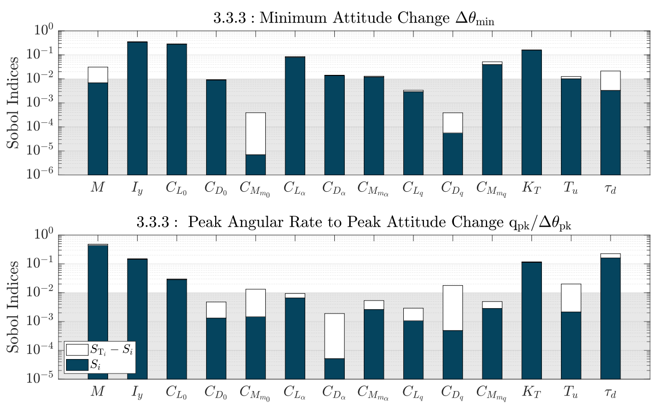

Figure 7. Attitude quickness, Sobol indices.

by M, K_T and τ_d, the second by C_{L_0}, I_y and $C_{M_{mq}}$ - confirming damping trends for aerodynamics - and a third combining α-derivatives, rotor speed dependency T_u and C_{L_q}.

The Sobol' indices in Figure 12 confirm the MOAT findings, reasserting the relevance of C_{L_0} and $C_{M_{mq}}$, already highlighted in the quickness simulations.

Figure 13 illustrates that the aircraft operates near the boundary between Level 1/2 established in (Ref. 5) for helicopters. Although the damping fluctuates around $\zeta = 0.35$ by approximately $\pm$ 0.05, the frequency shows much greater variability and significantly exceeds helicopter values, with $\omega_n = 5.61$ rad/s corresponding to a natural oscillation frequency of 0.9 Hz. This represents a very high frequency and is again attributed to the small size of the vehicle compared with the size of a manned helicopter.

Short-Term Response to Pitch Control Inputs

The last pHQ analysed is the bandwidth described in Section 3.3.2.1 of (Ref. 5), which investigates the behaviour of the

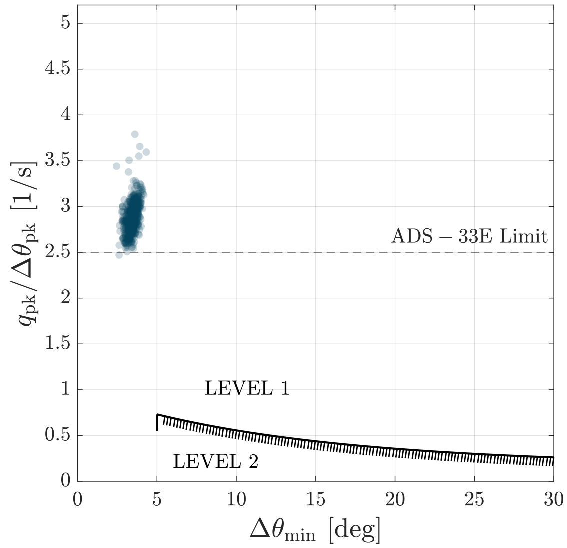

Figure 8. Attitude quickness ADS-33 MC results.

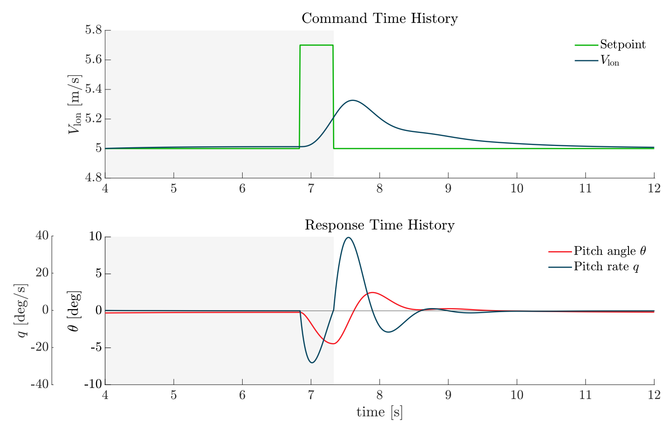

Figure 9. Dynamic Stability test manoeuvre.

aircraft in the frequency domain "to determine if there is sufficient phase margin to allow the pilot to close the attitude loop [...] without threatening stability" and to understand if the aircraft is PIO prone. The test used requires a longitudinal frequency sweep input and recording of the q-response, processed using the Fast Fourier Transform algorithm (FFT) to obtain Bode plots and evaluate the bandwidth ω_{BW} and the phase delay τ_p. Following (Ref. 29), a 90s automated sweep is generated, linearly increasing from 0.3 rad/s to 12 rad/s (approximately 0.05 Hz to 2 Hz). The ADS-33 test guide also suggests recording 20s before and after the sweep. Figure 14 illustrates the reference commands in the longitudinal speed and the related q-rate response.

However, performing a 130s simulation leads to inherently time-demanding computation to obtain the QoIs, making the UA prohibitively expensive. So, instead of analysing the complete nonlinear response, the criterion is applied to a linearised form of the FSM near a $V_{\text{lon}} = 5$ m/s trim point, reducing

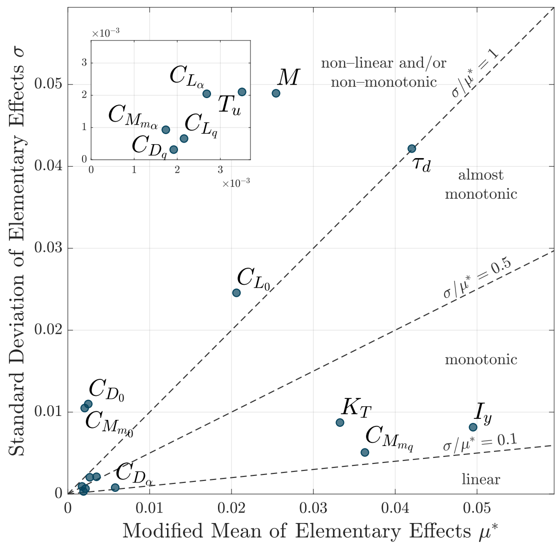

Figure 10. MOAT ζ.

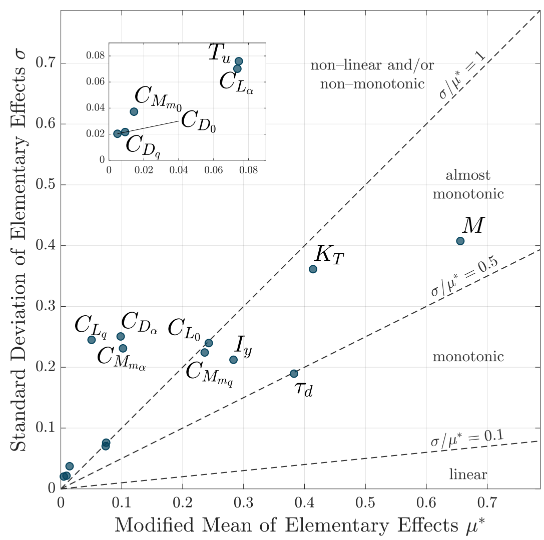

Figure 11. MOAT ω_n.

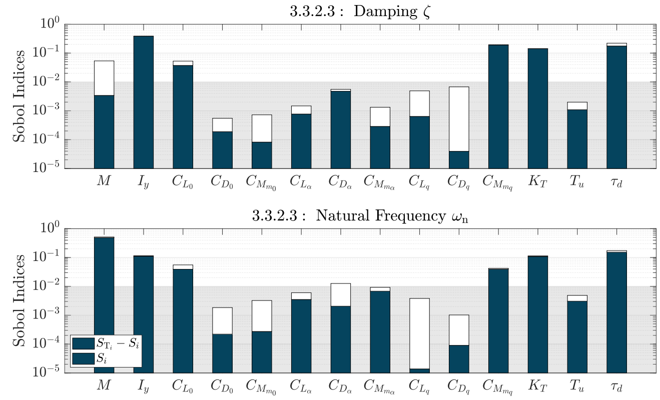

Figure 12. Dynamic Stability, Sobol indices.

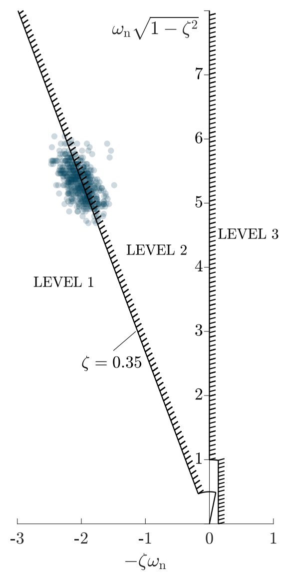

Figure 13. Dynamic stability ADS-33 MC results.

the computational costs but still capturing the main trends in bandwidth behaviour. Figure 15 compares the Bode plots obtained by the frequency sweep with those of the linearised system. It should be noted that the agreement between the models holds as long as the sweep applied to the nonlinear model stays within reasonably small amplitudes (Figure 15 has been derived from a $\Delta V_\mathrm{lon} = \pm 0.1$ m/s, resulting in $|\Delta\theta| < 1$ deg; up to $|\Delta\theta| \approx 5$ deg). As the applied sweep amplitude increases, differences may arise. A coherence plot is also shown for the FFT-based results. (Ref. 29) indicates a minimum value of 0.6 for the coherence to check the goodness of the sweep results. As specified in (Ref. 5), since the phase is nonlinear between the crossover frequency ω_{180} and $2\omega_{180}$, the phase delay τ_p must be determined by a linear least squares fit.

Unlike the other pHQs, the bandwidth results are much less variant (see Figures 16 and 17). This is reflected in both the MOAT analyses - featuring extremely small σ-values, which make most of the uncertain inputs fall into the linear/monotonic area - and in the VBD (Figure 18), where Sobol' indices are mainly composed of first-order effects. Apart from M - responsible for most of the output variance — three subgroups are identified. The first is again composed of C_{L_0} and $C_{M_{mq}}$, together with K_T and I_y. These factors contribute to $\omega_{BW_\mathrm{phase}}$ with Sobol' indices varying between values of 0.05 and 0.1. The second subset group is composed of α-derivatives, T_u and τ_d, and shows values less relevant but close to the threshold. The third group contains irrelevant factors. τ_p (Figure 17) exhibits a joint participation of all factors, as seen for $\Delta\theta_\mathrm{min}$ in the Attitude Quickness requirement, with an increased importance played by aerodynamics. Figure 18 shows the Sobol' indices, again in agreement with MOAT μ^*.

The results of the bandwidth and phase delay UA are finally compared with the ADS-33 design limits defined for helicopters in Figure 19. A cluster of points exists at a significant distance from the threshold between the levels. $\omega_{BW_\mathrm{phase}}$ shows a wider range of variability than τ_p. The Bode phase

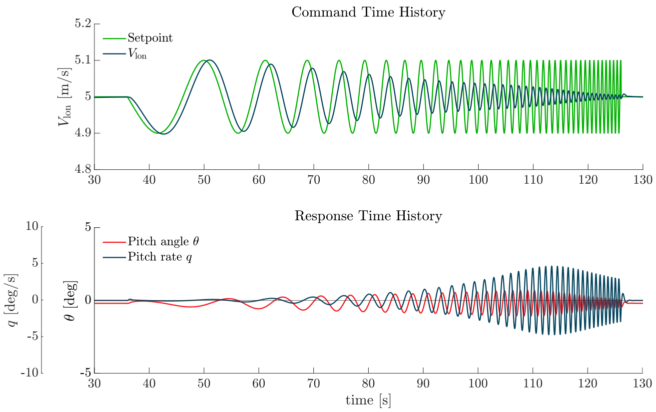

Figure 14. Bandwidth test manoeuvre.

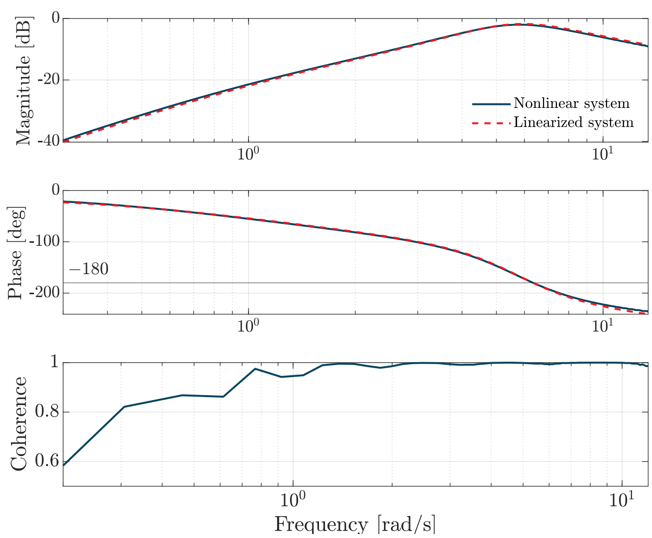

Figure 15. Bode plots for $q/\Delta V_{\mathrm{lon}}$.

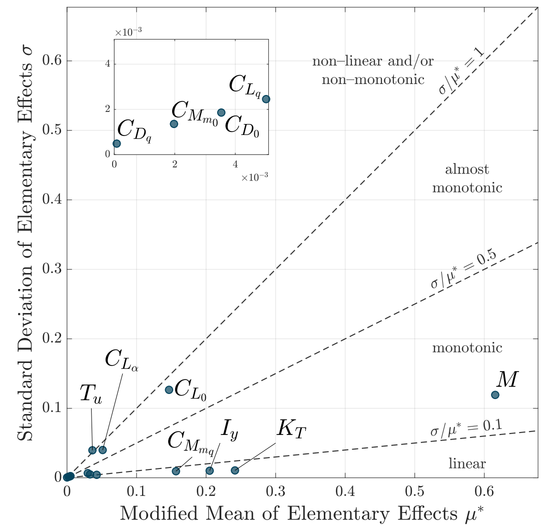

Figure 16. MOAT ω_{BW}.

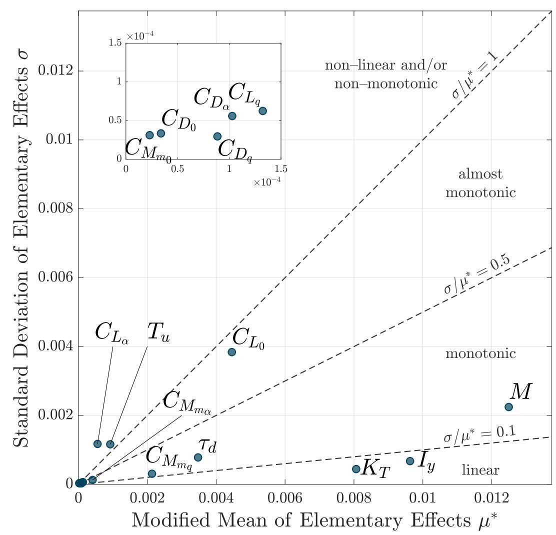

Figure 17. MOAT τ_d.

curve of the uncertain models showed a greater variation in the range between bandwidth and crossover frequency (ω_{180}), shifting bandwidth values throughout 4–5 rad/s. Since the phase curve is less sensitive to variations for $\omega > \omega_{180}$, τ_p instead remained almost unchanged after ω_{180}, resulting in a much lower variance in the phase delay results.

In summary, it is possible to say that the UA analysis could be used effectively to identify the most relevant factors that influence the input uncertainty in terms of the selected pHQs. The efficient MOAT analysis was very effective in identifying the relevant factors, providing results very close to those obtained by the more demanding VBD analysis. Then MC results, mainly extracted from analysis already used to determine the VBD, could be used to assess the uncertainty of the FSM in the space of pHQ.

VERIFICATION OF THE IMPACT OF UNCERTAINTIES ON ASSIGNED HQS THROUGH THE EVALUATION OF FTMS

To assess whether the uncertain models identified through the previous Uncertainty Analysis (UA) also correspond to those causing the largest variations in the performance parameters for the assigned HQ case under investigation, we analyse the responses of several of the most critical uncertain cases during a deceleration-to-hover manoeuvre. In principle, these tests must be performed considering the presence of a pilot in the loop, since a real pilot will probably adapt the piloting strategy while perceiving a change in the aircraft dynamic behaviour. However, since we are only interested here in the potential impact of model input uncertainties on the aHQs, we will simply perform the simulation closing all control loops of the flight controller of the aircraft and checking *de facto* if the same virtual pilot, without strategy adaptation, is still able to control

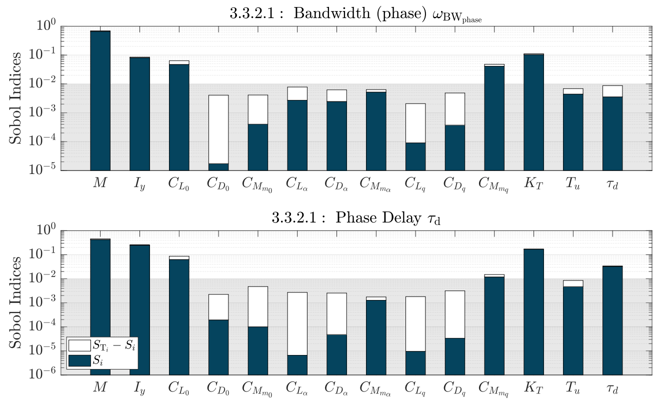

Figure 18. Bandwidth, Sobol indices.

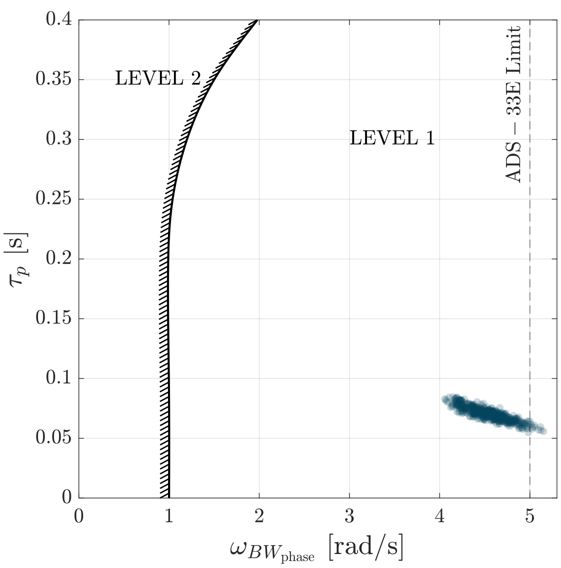

Figure 19. Bandwidth ADS-33 MC results.

the aircraft and keep the same desired/adequate performance of the nominal model.

Selection of Test Points

At this stage, the focus shifts to the assigned dimension of the HQs. The main objective of this section is to execute the selected FTM to collect the HQ evidence required by the MHQRM (Ref. 1). Exploiting the UA results, a series of uncertain aircraft configurations is selected from the MC output dataset for the execution of the FTM. Two sets of HQ tests are presented: the first is carried out in the normal flight envelope (NFE) (the NFE "*corresponds to the normal use of the VTOL aircraft according to its concept of operations*" (Ref. 4)) in calm air. The second is still in the NFE but now operates with atmospheric disturbances and is tested with the intent of verifying how much the uncertainty impacts the evaluation with AD as required by (Ref. 1).

The approach presented here builds on the outcome of a previous study (Ref. 31). In that work, for each pHQ QoI, four equally spaced points were selected, starting from the mean value of each index and extending toward the extreme of the corresponding distribution in the "least favourable" direction—i.e., along either the abscissa or the ordinate of the pHQ maps (Ref. 5), in the direction which led to a degradation in the aircraft's HQR level.

Given that eight configurations were insufficient to adequately capture the impact of uncertainty in each pHQs on the aHQ performance and since these cannot be varied independently (i.e. without causing changes in the other pHQs), a new approach is introduced in this work. The core idea behind the proposed workflow is to select the test configurations that maximise the variance of the corresponding distribution: for each pHQ (i.e. attitude quickness, dynamic stability, bandwidth) the approach requires the execution of a Principal Component Analysis on the MC output distributions, after which 40 points are chosen moving along the identified First Principal Component (PC1), from one end of the distribution to the other. They are selected to be equally spaced in terms of their projection along the PC1-axis (whose coordinate is hereafter defined as η). The selection of a high number of test configurations is driven by the need to thoroughly explore the entire uncertain space, thus avoiding local solutions. Figure 20 shows an example of the selection process applied to the Attitude Quickness case (for better visualisation and to identify the PC1 direction, the same scale is used for both axes). Repeating the process for each pHQ, a total of 120 different configurations are tested.

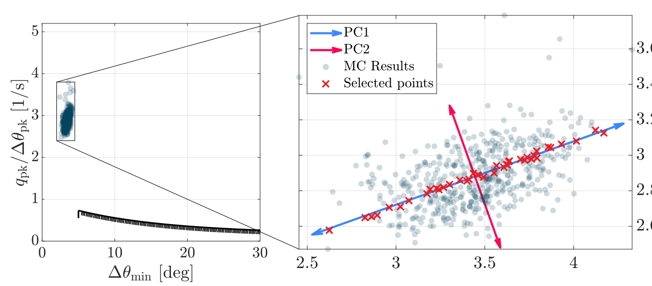

Figure 20. PCA-based test points selection procedure

The main advantage of the proposed approach is that the PC1 directions associated with the three different pHQs exhibit a high level of correlation. Specifically, the test configurations corresponding to points sampled from the MC distribution of one pHQ tend to produce, with respect to the other two , points that align along the PC1-axis of their respective distributions. In other words, the set of configurations yielding the largest variance in one pHQ-space tend to maximise the variance also for the other two pHQs. Moreover, the sign is preserved between pHQ-spaces, meaning that the worsening direction (i.e. the one that drives the aircraft towards the ADS-33 boundaries) is consistent across the distributions, for this set of selected pHQs. This ultimately allows for the identification of global deterioration - and, conversely, improvement - directions, both in orientation and sign in the Predicted dimension of HQs. Figure 21 shows how each set of selected points (identified in red) projects over the other two pHQ-spaces: despite a higher spread resulting from the points sampled from the Attitude Quickness space, high alignment is obtained for the projections involving Dynamic Stability and Bandwidth.

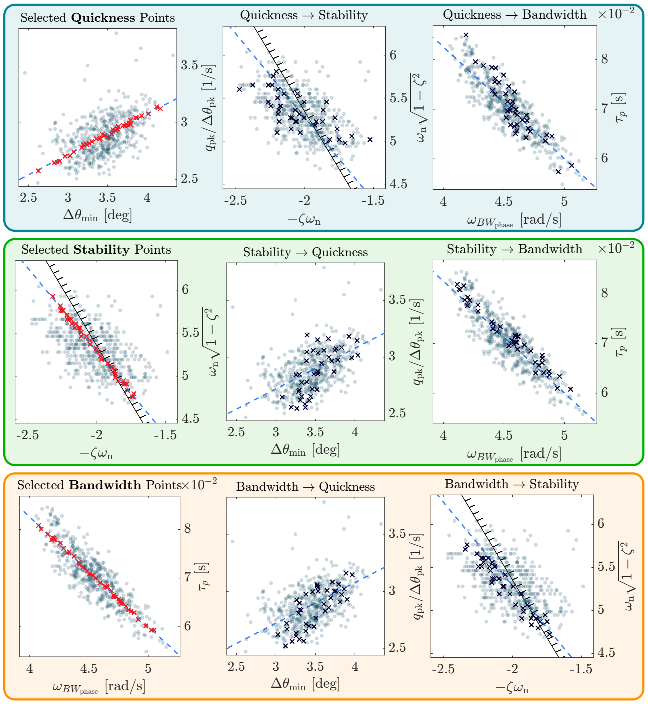

Figure 21. Selected configurations: Quickness (top), Stability (middle), Bandwidth (bottom). Red identifies the chosen ones, dark blue their projections between pHQs.

Normal Flight Envelope Results

Figure 22 shows the trajectories obtained by simulating the deceleration-to-hover manoeuvre with all the configurations presented in Figure 21, highlighting the deviations obtained for the lateral track, the heading, the altitude and the longitudinal position of the arrival point. First, it must be noted that the baseline configuration is not able to ensure Level 1 HQs due to the inability to stay within the desired limits for altitude, whose performance is the most affected by the uncertainty of the FSM. As Figure 22 shows, the eVTOL gains significant altitude during the FTM: at the start of the deceleration phase, the controller commands a sharp pitch-up manoeuvre to initiate braking. Due to the high aggressiveness of the command and the sustained forward speed at which the deceleration begins, the aircraft responds with a rapid climb. A similar effect occurs during acceleration, where the eVTOL loses altitude. However, since this phase starts from a hover, the impact is less marked.

In terms of lateral-directional performance, the vehicle comfortably achieves the desired level, with lateral track deviations and heading excursions remaining around the order of 10^{-2} throughout all simulations. This outcome directly reflects the findings of roll-due-to-pitch coupling, which con-

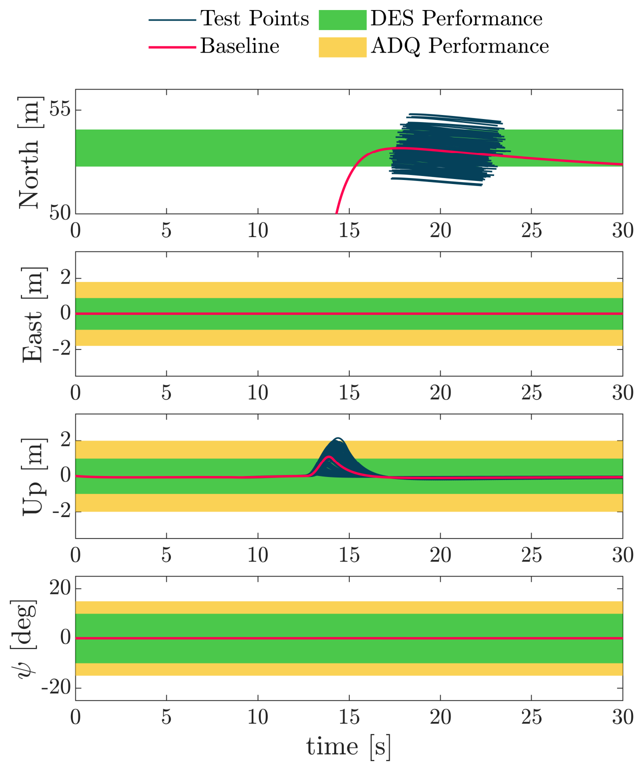

Figure 22. Recorded time histories of the NFE case. The four diagrams show the horizontal trajectory coordinate, the altitude and the azimuth angle. The coloured bands show the desired and adequate ranges.

firmed the absence of coupling when the aircraft is operated in a purely longitudinal manner. Regarding the longitudinal requirement, although the aircraft can maintain a stable hover for the expected duration, configuration uncertainties can result in minor deviations from the desired region.

To understand how the previously selected uncertain aircraft configurations translate into aHQ performance, the evolution of the task performances for each pHQ-set is analysed in Figure 23. Individual performance parameters are plotted against the η-coordinate for each set of 40 configurations, here normalised to the [0, 1] interval, with pHQ-Level gradually improving as η proceeds from 0 to 1. This allows for the identification, as previously stated, of global variation directions for the pHQs. Interestingly, despite major fluctuations in the curves, a monotonic change in the pHQs translates into clearly identifiable trends in task performance within the Assigned dimension of the HQs. Specifically, as the pHQs improve there is, on average, a corresponding enhancement in lateral, azimuthal and longitudinal performances. A more manoeuvrable, stable and controllable aircraft results indeed in significantly smaller deviations during the execution of the FTM, although this comes at the cost of a greater altitude gain following deceleration.

The analysis highlights two main outcomes.

- Firstly, aside from the altitude requirement, the FTM can

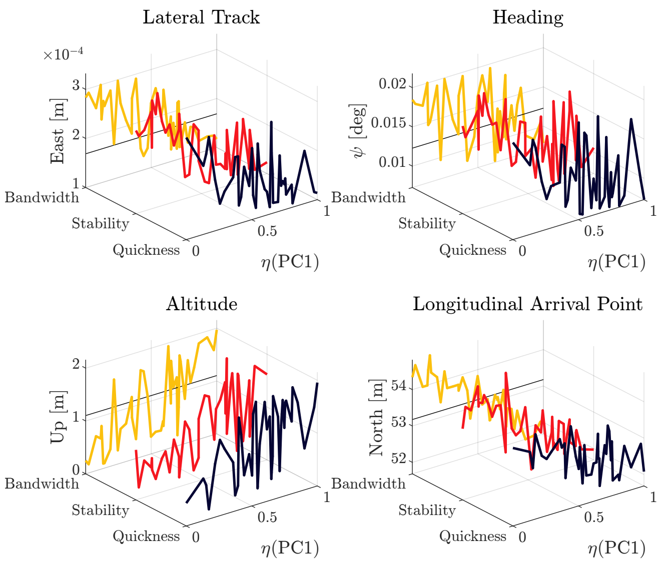

Figure 23. FTM results for the NFE case. Black lines identify baseline configuration's performances.

generally be completed at the desired level when flying in the NFE (i.e. in the absence of external disturbances). This is primarily due to the effectiveness of the FCS, which is capable - even under high attack rates - of keeping the eVTOL within the required boundaries, especially along the lateral-directional axes.

- Secondly, despite the positive contribution of the FCS to the closed-loop response of the aircraft, the uncertainty in the pHQs still has a significant impact on the overall FTM performance. This is even more evident in the case under analysis, where the initially selected pHQs are able to accurately capture variations in the performance parameters of FTM.

Overall, it is possible to say that parameter sets in the range of uncertainty that lead to worse pHQs also show a significant effect on the aHQ behaviour. So, the idea of performing the uncertainty assessment at the level of pHQs, using much simpler open-loop tests, represents a good approach for the identification of the most critical FSM. Still, as required by (Ref. 5), the overall HQ level shall result from a combination of Predicted and Assigned Levels. The results suggest that the level of uncertainty in the input models is large and consequently the impact on the aHQs is significant. So, it is possible to conclude that a lower uncertainty in the FSM input parameter will be necessary to employ only the nominal model in the aHQ simulations with confidence.

Atmospheric Disturbance Flight Test Results

The FTM operations are now extended to include the effect of atmospheric disturbances, entering an area of the flight envelope where the credibility of the FSM becomes crucial to assess HQ results—particularly because, under such conditions, flight test data would normally not be available or would be difficult to obtain. To analyse the VTOL behaviour under external disturbances, a wind turbulence model is introduced. The method adopted here follows MIL-F-8785C (Ref. 32) and the Von Kármán spectral model is used. The model defines the power spectral density for the three turbulent velocity components - taking white noise as input - and the turbulent roll angular rate spectrum; pitch and yaw rates are derived subsequently from the velocity components. In addition to random fluctuations, a mean wind component dependent only on altitude is applied.

In this study, headwind was chosen as the most critical, based on the results obtained in (Ref. 31). As Figure 24 shows, the performance parameter deviations due to model input uncertainties u_{inp} are significantly amplified in the presence of disturbances. The aircraft is no longer able to consistently meet the longitudinal requirement. Furthermore, during the 5 s hover phase, substantial deviations are observed from the intended arrival point (top-left plot in Figure 24), mainly due to wind effects during hover and the use of the multicopter controller's position mode. Enhancing position control during this phase may help maintain compliance with the requirement, allowing the aircraft to hold its intended arrival point. Heading performance also suffers a marked degradation, with the eVTOL exhibiting large ψ deviations once the deceleration ΔV_{lon} is commanded. This effect is primarily driven by the p-rate turbulence component, which, combined with lateral velocity v, strongly couples with the pitch and yaw axes. As a result, the aircraft frequently exceeds adequate boundaries. Figure 24 highlights how this issue becomes more prominent near the end of the deceleration phase, when the aircraft reaches its maximum pitch angle.

Figure 25 investigates the relationship between the evolution of the pHQs and the corresponding changes in the resulting aHQ performance. Even in the presence of atmospheric disturbances, clear improvements can still be seen in lateral and longitudinal performance, while heading performance appears to be masked by fluctuations. These gains, however, come at the cost of a noticeable degradation in altitude performance. Once again, the selected pHQs show a strong and consistent correlation with the resulting aHQs.

These results demonstrate that the simulation-based approach is effective in capturing the impact of atmospheric disturbances on vehicle HQs. Trends with wind intensity and direction are identifiable using the nominal FSM. These trends are reproduced similarly by the modified configurations; however, it must be remembered that the uncertainty levels considered have been assessed as large in the previous section.

MAXIMUM UNNOTICEABLE ADDED DYNAMICS

MUAD boundaries are defined as changes in aircraft dynamics that can be introduced without the pilot consciously perceiving them. The approach introduced earlier states that if

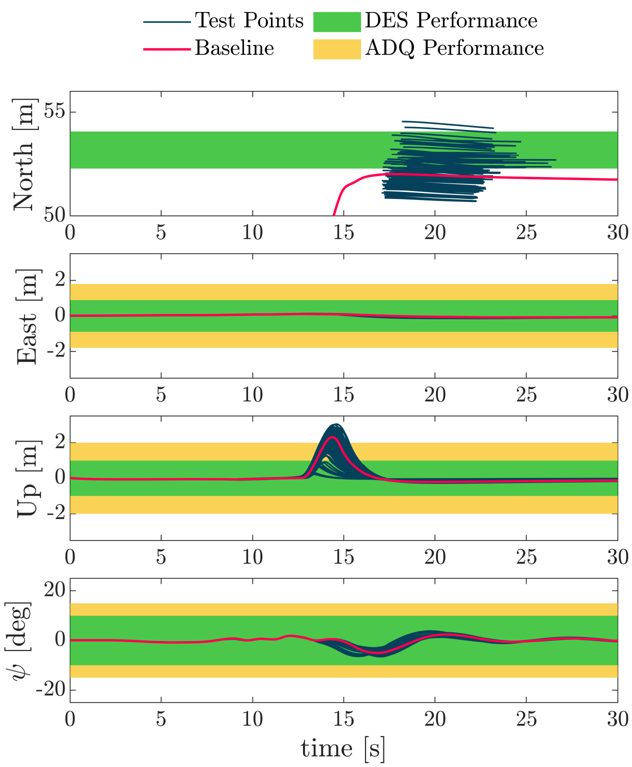

Figure 24. Recorded time histories under $V = 0.5$ m/s headwind.

the envelope of the uncertain transfer functions related to the ACR under analysis, scaled by the selected *CR*, falls within the MUAD limits, then the nominal model may be considered credible and used for ACR evaluations in flight simulators. In this work, the minimum acceptable *CR* is assumed to be 1 (Ref. 6). Conversely, if the uncertainty ranges surrounding the nominal results exceed the MUAD boundaries, the model should not be considered credible. In that case, the applicant must either reduce the uncertainty or assess its effect on the simulation outcomes. Initially developed in the context of fixed-wing aircraft handling qualities criteria (Ref. 33), MUAD boundaries have become a widely recognized tool for evaluating flight model fidelity, by serving as limits for acceptable model mismatch. Their use as fidelity criteria was first proposed in (Ref. 34). Although still unexplored for VTOLs and other novel configurations, their applicability to rotorcraft simulation fidelity has been discussed in the literature (Refs. 34–37). The envelopes (Table 4) are valid over the frequency range from 10^{-2} to 10^{2} rad/s and exhibit an "hourglass" shape, narrowing near 3 rad/s, the frequency region most relevant to manual control (Ref. 38).

In light of this, the MC-generated FSM can be employed to assess the influence u_{inp} has on the aircraft transfer function (TF), computing the envelope of uncertain TFs (eTFs) and comparing them with the nominal one. It must be clearly acknowledged that MUAD boundaries were originally conceived for a class of aircraft very different from eVTOLs and

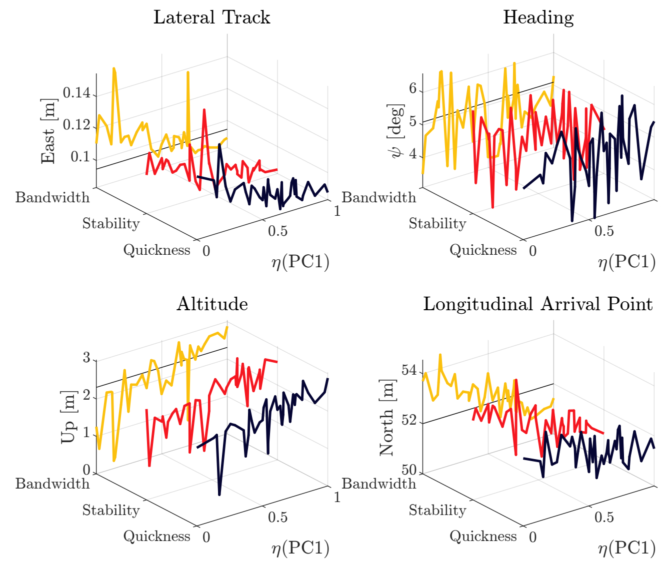

Figure 25. FTM results under $V = 0.5$ m/s headwind.

Table 4. MUAD Envelope Transfer Functions (Ref. 39).

Envelope Type	Transfer Function
Upper Gain	$\dfrac{3.16s^2+31.61s+22.79}{s^2+27.14s+1.84}$
Lower Gain	$\dfrac{0.0955s^2+9.92s+2.15}{s^2+11.60s+4.95}$
Upper Phase	$\dfrac{68.89s^2+1100.12s-275.22}{s^2+39.94s+9.99}e^{0.0059s}$
Lower Phase	$\dfrac{475.32s^2+184100s+29456.1}{s^2+11.66s+0.0389}e^{-0.0072s}$

may therefore have limitations in their applicability. A key contribution is provided by (Ref. 39), which reports an extensive simulator-based study for helicopter certification. The experiment investigated pilot sensitivity to variations in system dynamics during a demanding manual control task (specifically, a hover MTE). This led to the definition of a new set of simulation validation limits, named Allowable Error Envelopes, tailored to the vehicle's bandwidth, the simulation facility's characteristics and the piloted task under consideration. In this work, however, the original MUAD boundaries are deliberately used to demonstrate the proposed method for enhancing FSM credibility. A sensitivity analysis was also performed to evaluate how various added dynamics affect the VTOL model, accounting for vehicle's frequency-dependent dynamic behaviour during the selected FTM.

In Figure 26 below, the main outcome of this first MUAD assessment is shown. The nominal system $q/\Delta V_{\text{lon}}$ Bode plots are displayed together with their uncertain region - derived using the MC results of the UA phase - and the corresponding "added-dynamics interpretation" is given (Figure 27). The difference between the 500 MC output eTFs and the reference TF is interpreted as unmodelled dynamics, showing that the uncertainty leading to the eTFs is bounded by MUAD limits for all the relevant frequencies (0.3-12 rad/s), except for some limited excursion outside magnitude boundaries slightly above 6 rad/s. It can therefore be reasonably assumed that the FTM results obtained using the baseline FSM configuration would yield similar HQ ratings to both the worst and best cases within the uncertainty range, at least for those performance aspects governed by this TF. According to the proposed approach, these results align with those obtained in the NFE. The differences between configurations are not significant enough to push the eTFs outside the MUAD envelope for this TF , even if the uncertainties in the model input parameters were assumed as relatively large.

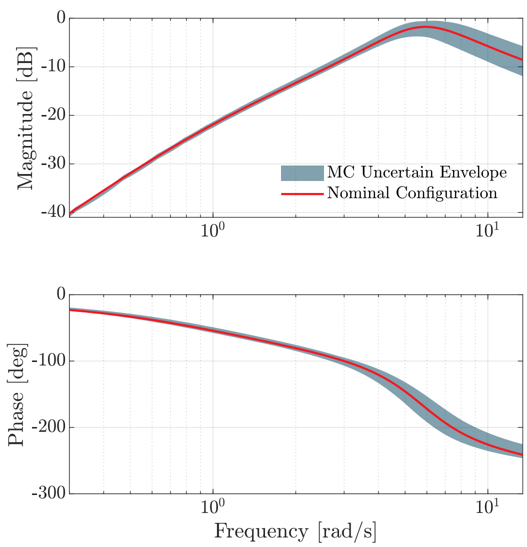

Figure 26. MC uncertain Bode plots envelope for $q/\Delta V_{\mathrm{lon}}$.

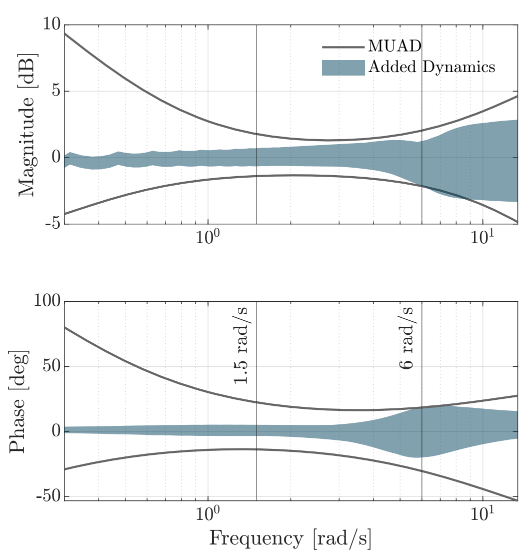

Figure 27. Equivalent added dynamics for $q/\Delta V_{\mathrm{lon}}$, compared against MUAD bounds.

Following a similar line of reasoning, the previous altitude performance results can be interpreted in MUAD terms. The FTM simulation phase highlighted indeed an increased altitude gain in the VTOL's response, revealing a strong coupling between the longitudinal and vertical axes in the assigned dimension of the HQs. Therefore, it is necessary to investigate whether this behaviour may be attributed to the shape of the added dynamics related to input uncertainties. To explore this aspect, the eTFs between the longitudinal input command and the resulting vertical velocity response $V_z/\Delta V_{\mathrm{lon}}$ ($X_z/\Delta V_{\mathrm{lon}}$ analysis yields analogous results) are computed and the corresponding added dynamics are examined (Figure 28). Several configurations exceed the magnitude boundaries, particularly in the mid-frequency range where the system is more sensitive. The broader spread of the worst TFs correlates with the observed degradation in altitude performance, resulting in greater variability in FTM outcomes, as shown in Figure 22. Although not all critical configurations identified in Figure 21 lie outside the MUAD envelope - highlighting the need for a sufficiently complete pHQ set in the UQ phase - several edge cases in the η interval do exceed the limits, particularly for attitude quickness and dynamic stability. This further supports the validity and potential of the proposed approach.

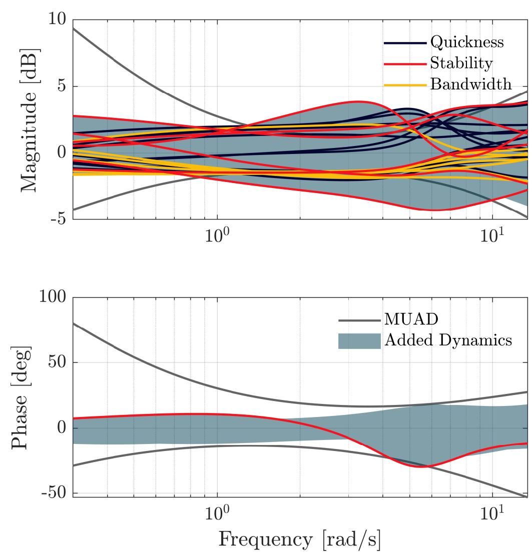

Figure 28. Equivalent added dynamics for $V_z/\Delta V_{\mathrm{lon}}$, compared against MUAD bounds. Coloured lines identify configurations exceeding MUAD limits.

Once this first assessment has been carried out, the sensitivity of the FSM to added dynamics across the frequency range can be studied, selectively assessing the validity of original MUAD boundaries on its dynamics. This process, which has been widely studied in the literature (Refs. 39–41), requires us to investigate the aircraft response to several added dynamics, specifically tailored to modify the baseline transfer function at several frequency values. This allows exploring the pilot control sensitivity and adaptation in terms of the HQ rating. The simplest approach to perturb the transfer function is to model the added dynamics H_{add} either as first-order lag-lead and lead-lag dynamics, as in (Ref. 40), or through second-order dynamics in the form of dipoles (Refs. 39, 41).

$$H_{\text{add}}(s) = \frac{s^2 + 2\omega_{dp}\zeta_z s + \omega_{dp}^2}{s^2 + 2\omega_{dp}\zeta_p s + \omega_{dp}^2}. \quad (4)$$

This work employs the second-order form, as it allows us to intuitively control the frequency position of the disturbance and gradually increase/decrease the corresponding amplitude. To preserve the shape of H_{add} within the control loop, the dipole is placed in series with the controller's velocity set-point ΔV_{lon}. Following the approach discussed in (Ref. 41), ω_{dp} was relocated iteratively between 1 and 6 rad/s, while ζ_z was gradually increased from 0.25 to 0.70. The damping ratio of the denominator was always fixed at $\zeta_p = 0.2$. Figure 29 shows an example of the adopted approach.

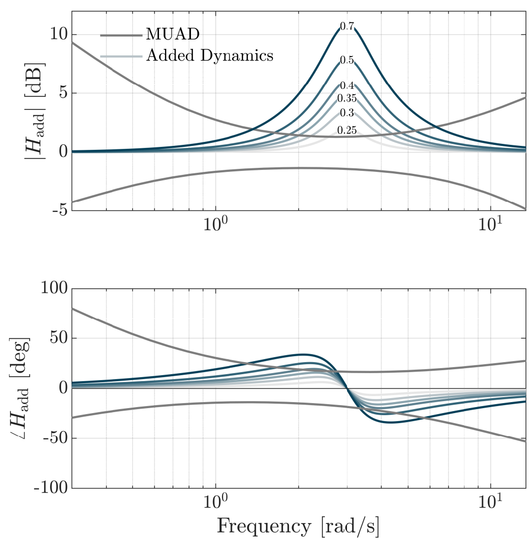

Figure 29. Bode plot of added dynamics for varying ζ_z (0.25–0.70).

To plan the FTM simulations, three flight conditions were analysed: the case of NFE operations ($V_{\text{wind}} = 0$ m/s) and the cases of headwind ($\psi_{\text{wind}} = 0°$) for both $V_{\text{wind}} = 0.5$ m/s and $V_{\text{wind}} = 1$ m/s. Figure 30 collects the results for altitude performance, which is the most sensitive to variations in H_{add}. For all of the tested operating conditions, a clear dependency upon the dipole's location exists. While in the high part of the frequency range ($\omega \geq 3$ rad/s), the H_{add} effect is not driving the rating out of the baseline level, at lower frequencies (in the range 1.5-3 rad/s), the results show the greatest variability, eventually bringing the system outside the adequate boundary. It can also be observed that while at high frequencies the trend of the performance decreases monotonically with increasing the frequency of ω_{dp} and increases monotonically with the intensity of the added disturbance (i.e., with ζ_z), at low frequencies this monotonicity is lost.

This behaviour can be attributed to two main factors. The first reason can be sought in the effect H_{add} exerts on ΔV_{lon}. When a high-ζ_z low-frequency dynamics is inserted within the control loop, the dynamics of the aircraft is affected to such an extent that the velocity command is inhibited. As a result, the aircraft can no longer adequately follow the input imposed by the controller, leading to oscillations in both the input and the response that disrupt the FTM. In this context, the observed improvement, visible at 1 and 2 rad/s in Figure 30, should not be interpreted as a beneficial effect of the added dynamics but rather as a consequence of the piloting algorithm's inability to correctly manoeuvre, ultimately making the results unreliable. Specifically, during the acceleration phase, the eVTOL reaches the required maximum forward speed much more slowly than in the nominal case, drastically reducing the level of aggressiveness needed for the manoeuvre and both the deceleration aggressiveness and the associated altitude gain. So, the improvement in altitude performance does not correspond to an overall improvement in the FTM performance. A second interpretation can be sought, like the HQ requirement assigned to the aircraft, as the required FTM input does not contain any high-frequency component and is likely to be mostly affected by dipoles located in the lower part of the frequency range. A different task (e.g., a *pitch-tracking* task for the measurement of control effort, as performed in (Ref. 41)) may result in a different frequency-related behaviour. It is interesting to note that as the H_{add} vary and, specifically, as the bandwidth parameter decreases (i.e., approaching the threshold between Level 1 and Level 2 of ADS-33), the degradation in the pHQs, now directly controlled using the added TF - rather than indirectly influenced via different aircraft configurations - directly translates into a deterioration in the corresponding assigned HQs, further supporting the results of Figure 23.

In summary, this analysis showed that taking the envelope of uncertain models in the frequency domain and comparing it with MUAD limits may be a good way to verify if the uncertainties are able to generate modifications that can affect or not the aHQ performance. However, it is important to consider uncertainties that affect a complete set of pHQs and compare all direct and cross-transfer functions that affect the FTM with the MUAD limits.

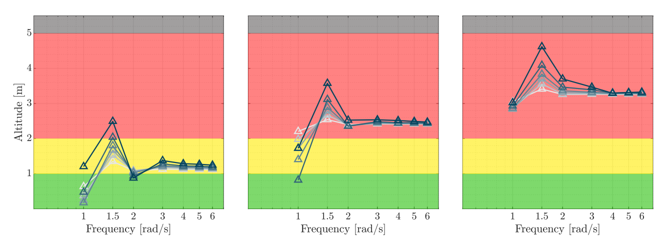

Figure 30. Results for varying H_{add}: no wind (left), $V_{\text{wind}} =$ 0.5 m/s (centre), $V_{\text{wind}} = 1$ m/s (right).

CONCLUSIONS

This paper successfully proposed and demonstrated a methodology for assessing the credibility of flight simulation models for VTOL handling qualities certification by simulation. The key results obtained are:

- The impact of FSM input parameter uncertainties was effectively propagated through sensitivity analysis (MOAT, VBD) to quantify variations in open-loop predicted HQs and, subsequently, in the aircraft's envelope of transfer functions.
- Selecting FSM configurations along the Principal First Component of the predicted HQ distribution shows that high variance in one pHQ typically aligns with high variance in the others. The pHQs also correlate with performance metrics associated with the assigned HQs: as pHQs improve, so does lateral, azimuthal, and longitudinal performance. The result is a more stable and controllable aircraft with reduced deviations during the FTM—although the altitude gain during deceleration increases. This confirms the suitability of the chosen pHQs to support the assigned HQs.
- A novel application of the Maximum Unnoticeable Added Dynamics concept was introduced: by comparing the envelope of uncertain TFs, scaled by a confidence ratio, against MUAD boundaries, a quantitative criterion for FSM credibility for specific HQ-related tasks was established.

For the studied lift+cruise VTOL model and the deceleration to hover flight test manoeuvre, the eTFs for longitudinal control dynamics largely satisfied the MUAD limits across the uncertain configurations, suggesting that the nominal FSM is credible for assessing performance aspects primarily driven by these dynamics. However, the eTFs for vertical axis dynamics coupled with longitudinal inputs for several uncertain configurations exceeded the MUAD magnitude limits. This finding correlated well with the observed variability and degradation in FTM altitude-keeping performance, indicating that FSM uncertainty in these coupled dynamics could lead to non-credible predictions for altitude-critical tasks if the nominal model alone were used.

The deliberate introduction of added dynamics in the form of dipoles further confirmed the frequency-dependent sensitivity of FTM performance, particularly altitude control, to deviations from the nominal aircraft dynamics.

These findings are highly promising for the advancement of a standardised certification by simulation approach for VTOL aircraft. The MUAD-based framework offers an objective, engineering-driven method to link FSM fidelity directly to pilot-perceptible dynamic changes. This is a significant step towards reducing reliance on extensive and potentially hazardous flight testing, especially when evaluating off-nominal conditions or the impact of model uncertainties. By demonstrating that an FSM's predictions remain within "unnoticeable" dynamic boundaries despite its uncertainties, confidence in its use for certification can be substantially increased.

It must be noted that this is a first attempt to identify a methodology for credibility assessment of VTOL models. More cases should be analysed in the future to fully verify if it is applicable as is to all VTOL configurations and all possible FTMs, or if further developments will be necessary.

Additionally, to fully mature this approach into a standardised practice, further investigation is crucial in several areas:

- Development of VTOL-Specific Requirements: the analysis of the Deceleration-to-Hover manoeuvre revealed an uncontrollable altitude increase. While this issue is captured and constrained in the aHQ dimension, it is not addressed by any specific pHQ requirement. Developing a new metric at the pHQ level, such as altitude-pitch coupling, tailored to capture this type of handling quality deficiency, could therefore be beneficial.
- VTOL-Specific MUAD Boundaries: The existing MUAD boundaries were originally conceived for conventional aircraft. Research is needed to tailor, refine, and validate these boundaries for the diverse range of VTOL configurations (e.g., lift+cruise, multicopter, tiltrotor) and their unique critical flight tasks and control strategies.
- Comprehensive Transfer Function Assessment: although this study focused on key longitudinal and coupled vertical dynamics, a standardised approach would require a systematic assessment of all relevant direct and cross-coupling transfer functions that significantly influence critical FTM performance against MUAD limits.

Addressing these areas will make the proposed CbS methodology more robust, paving the way for more efficient, cost-effective certification pathways for the rapidly evolving VTOL aircraft sector.

Author contact:
Lorenzo Favaro lorenzo.favaro@polimi.it
Agata Rylko agata.rylko@polimi.it
Giuseppe Quaranta giuseppe.quaranta@polimi.it

ACKNOWLEDGMENTS

The work in this study performed by Agata Rylko was carried out within the 38th cycle of doctoral study in aerospace engineering, in the research field "Policymaking for Urban Air Mobility acceptance" and received funding from PIANO NAZIONALE DI RIPRESA E RESILIENZA (PNRR). The work in this study performed by Giuseppe Quaranta and Lorenzo Favaro was carried out within MOST-–Sustainable Mobility National Research Center and received funding from the European Union Next-Generation EU (PIANO NAZIONALE DI RIPRESA E RESILIENZA (PNRR)–MISSIONE 4 COMPONENTE 2, INVESTIMENTO 1.4–D.D. 1033 17/06/2022, CN00000023).

REFERENCES

1. Anon., "Third Publication of Means of Compliance with Special Condition VTOL, MOC-3 SC-VTOL Issue 2", EASA, Cologne, Germany, 2023.

2. Anon., "SC-VTOL, Special Condition for Small-Category VTOL Aircraft, Issue 1," EASA, Cologne, Germany, 2019.

3. Cooper, G. E., and Harper, R. P., "The Use of Pilot Rating in the Evaluation of Aircraft Handling Qualities," NASA US Department of Defense Interface Standard TN D-5153, 1969.

4. Anon., "ED-295, Guidance on VTOL Flight Control Handling Qualities Verification," EUROCAE, Saint Denise, France 2024.

5. Anon., "MIL-DTL-32742(AR)," Department of Defense Detail Specification Handling Qualities for Military Rotorcraft, Redstone Arsenal, AL, USA, 2023.

6. Padfield, G., and van't Hoff, S., and Hofmeister, P., and Lu, L., and White, M., and Quaranta, G., *Rotorcraft Certification by Simulation and Analysis. An Introduction to the Principles and Practices*, Springer, Cham, Switzerland, 2025. DOI: 10.1007/978-3-031-86398-1.

7. Bianco-Mengotti, R., and Ragazzi, A., and Del Grande, F., and Cito, G., and Brusa Zappellini, A., "AW189 Engine-Off-Landing Certification by Simulation", American Helicopter Society 72nd Annual Forum, West Palm Beach, FL, USA, May 2016.

8. Ragazzi, A., and Bianco-Mengotti, R., and Sabato, P., and Afruni, G., and Hyder, C., "AW169 loss of tail rotor effectiveness simulation", 43th European Rotorcraft Forum, Milano, Italy, September 2017.

9. Pedrioli, A., and Vaiuso, A., and Pedrazzini, N., and Coretti, O., and Sanchez, G. E., and Pinsard, L., and Gomes, J. V., and Capone, L., and Righi, M., "Flight Simulation Model of a Multi-Fidelity Digital Twin of an eVTOL Drone", 50th European Rotorcraft Forum, Marseille, France, September 2024.

10. Roussas, G. G., *A Course in Mathematical Statistics*, Elsevier, Amsterdam, The Netherlands, 1997.

11. Elishakoff, I., *Safety Factors and Reliability: Friends or Foes?* Springer Science & Business Media, Dordrecht, The Netherlands, 2004.

12. Wilson, D., and Riley, D., "Cooper-Harper pilot rating variability", AIAA 16th Atmospheric Flight Mechanics Conference, Boston, MA, USA, August 1989. DOI: 10.2514/6.1989-3358.

13. Anon., "Flying Qualities of Piloted Aircraft," Technical Report MIL-STD-1797A, US Department of Defense Interface Standard, 1990.

14. Martello, N. C., "Modelling and Integration of an eVTOL UAV," Master's Thesis, Politecnico di Milano, Milano, Italy, 2021.

15. Martinelli, E., "Modelling, Control, Integration and Testing of an eVTOL Drone," Master's Thesis, Politecnico di Milano, Milano, Italy, 2022.

16. Bara, K., "Aerodynamics, Propulsion and Testing of an eVTOL Drone," Master's Thesis, Politecnico di Milano, Milano, Italy, 2023.

17. Rylko, A., and Lovera, M., and Quaranta, G., "Aerodynamic Model Development and Fidelity Assessment for eVTOL Predicted Handling Qualities", 50th European Rotorcraft Forum, Marseille, France, September, 2024.

18. Tobias, E. L., and Tischler, M. B., "A Model Stitching Architecture for Continuous Full Flight-Envelope Simulation of Fixed-Wing Aircraft and Rotorcraft from Discrete-Point Linear Models," Technical Report Special Report RDMR-AF-16-01, US Army AMRDEC, Huntsville, AL, USA, 2016.

19. Nabi, H. N., and de Visser, C. C., and Pavel, M. D., and Quaranta, G., "Development of a quasi-linear parameter varying model for a tiltrotor aircraft", *CEAS Aeronautical Journal*, Vol. 12, September 2021, pp. 879–894. DOI: 10.1007/s13272-021-00539-1.

20. Dalbey, K., and Eldred, M., and Geraci, G., and Jakeman, J., and Maupin, K., and Monschke, J., and Seidl, D., and Swiler, L., and Tran, A., and Menhorn, F., *Dakota, A Multilevel Parallel Object-Oriented Framework for Design Optimization, Parameter Estimation, Uncertainty Quantification, and Sensitivity Analysis: Version 6.14 Theory Manual*, Sandia National Laboratories, Albuquerque, NM, USA, 2021.

21. Gentle, J. E., *Random Number Generation and Monte Carlo Methods*, Springer, New York, NY, USA, 2003.

22. Saltelli, A., and Ratto, M., and Andres, T., and Campolongo, F., and Cariboni, J., and Gatelli, D., and Saisana, M., and Tarantola, S., *Global Sensitivity Analysis*, Wiley, Hoboken, NJ, USA, 2008.

23. Campolongo, F., and Saltelli, A., "Sensitivity analysis of an environmental model: An application of different analysis methods", *Reliability Engineering & System Safety*, Vol. 57, (1), July 1997, pp. 49–69. DOI: 10.1016/S0951-8320(97)00021-5.

24. Anon., *ASME V&V 20 Standard for Verification and Validation in Computational Fluid Dynamics and Heat Transfer*, American Society of Mechanical Engineers, New York, NY, USA, 2009.

25. Morris, M. D., "Factorial sampling plans for preliminary computational experiments", *Technometrics*, Vol. 33, (2), May 1991, pp. 161–174. DOI: 10.2307/1269043.

26. Adams, B., and Bohnhoff, W., and Dalbey, K., and Ebeida, M., and Eddy, J., and Eldred, M., and Hooper,

R., and Hough, P., and Hu, K., and Jakeman, J., *Dakota, A Multilevel Parallel Object-Oriented Framework for Design Optimization, Parameter Estimation, Uncertainty Quantification, and Sensitivity Analysis: Version 6.16 User's Manual*, Sandia National Laboratories, Albuquerque, NM, USA, 2022.

27. Anon., "Proposed Revisions to Aeronautical Design Standard–33E (ADS-33E-PRF) Toward ADS-33F-PRF", U.S. Army Combat Capabilities Development Command, Redstone Arsenal, AL, USA, 2019.

28. Pavel, M., and Padfield, G., "Progress in the development of complementary handling and loading metrics for ADS-33 manoeuvres", American Helicopter Society 59th Annual Forum, Phoenix, AZ, USA, May 2003.

29. Anon., "Test Guide for ADS-33E-PRF," U.S. Army Research, Development, and Engineering Command, Moffet Field, CA, USA, 2008.

30. Menberg, K., and Heo, Y., and Choudhary, R., "Sensitivity analysis methods for building energy models: Comparing computational costs and extractable information", *Energy and Buildings*, Vol. 133, December 2016, pp. 433–445. DOI: 10.1016/j.enbuild.2016.10.00.

31. Favaro, L., and Rylko, A., and Quaranta, G., "Bulding Credible VTOL Flight Models for Handling Quality Certification by Simulation", *Aerospace*, Vol. 12, (6), June 2025. DOI: 10.3390/aerospace12060559.

32. Anon., "Background Information and User Guide for MIL-F-878SC, Military Specification - Flying Qualities of Piloted Airplanes," Air Force Wright Aeronautical Laboratories, Air Force Systems Command, Wright-Patterson Air Force Base, OH, USA, 1982.

33. Wood, J., and Hodgkinson, J., and Jenny, R., and Mello, J., "Definition of Acceptable Levels of Mismatch for Equivalent Systems of Augmented CTOL Aircraft," Defense Technical Information Center, Fort Belvoir, VA, USA, 1980.

34. Tischler, M. B., "System Identification Methods for Aircraft Flight Control Development and Validation," NASA Technical Memorandum 110369, 1995.

35. Tishler, M. B., and White, M., "Rotorcraft Flight Simulation Model Fidelity Improvement and Assessment. Final report of NATO STO AVT-296 Research Task Group," Technical report, NATO Science & Technology Organization, Brussels, Belgium, 2021.

36. Pavel, M. D., and White, M., Padfield, G., Roth, G., Hamers, M., Taghizad, A., "Validation of mathematical models for helicopter flight simulators. Past, present and future challenges", *The Aeronautical Journal*, Vol. 117, (90), April 2013, pp. 343–388. DOI: 10.1017/S0001924000008058.

37. Miletović, I., "Motion Cueing Fidelity in Rotorcraft Flight Simulation. A New Perspective using Modal Analysis," Doctoral Dissertation, Delft University of Technology, Delft, The Netherlands, 2020. DOI: 10.4233/uuid:4fdea178-a5b1-4620-987e-b1f2f9c23d32.

38. McRuer, D., and Jex, H., "A Review of Quasi-Linear Pilot Models", *IEEE Transactions on Human Factors in Electronics*, Vol. HFE-8, (3), September 1967, pp. 231–249. DOI: 10.1109/THFE.1967.234304.

39. Mitchell, D., and He, C., and Strope, K., "Determination of Maximum Unnoticeable Added Dynamics", AIAA Atmospheric Flight Mechanics Conference and Exhibit, Keystone, CO, USA, August 2006.

40. Butijn, M., and Lu, T., and Pool, D., and van Paassen, M., "Assessment of Maximum Unnoticeable Added Lag-Lead or Lead-Lag Dynamics with a Cybernetic Approach", AIAA Scitech Forum, San Diego, CA, USA, January 2019.

41. Matamoros, I., and Lu, T., and van Paassen, M., and Pool, D., "A Cybernetic Analysis of Maximum Unnoticeable Added Dynamics for Different Baseline Controlled Systems", *IFAC-PapersOnLine*, Vol. 50, (1), July 2017, pp. 15847–15852. DOI: 10.1016/j.ifacol.2017.08.2328.